Homologous series of layered structures in binary and ternary Bi-Sb-Te-Se systems: *Ab initio* study

K. Govaerts,[1,*] M. H. F. Sluiter,[2] B. Partoens,[3] and D. Lamoen[1]

[1]*EMAT, Universiteit Antwerpen, Groenenborgerlaan 171, 2020 Antwerpen, Belgium*

[2]*Department of Materials Science and Engineering, 3mE, Delft University of Technology, Mekelweg 2, 2628 CD, Delft, The Netherlands*

[3]*CMT group, Department of Physics, Universiteit Antwerpen, Groenenborgerlaan 171, 2020 Antwerpen, Belgium*

(Received 12 September 2013; revised manuscript received 13 February 2014; published 28 February 2014)

In order to account explicitly for the existence of long-periodic layered structures and the strong structural relaxations in the most common binary and ternary alloys of the Bi-Sb-Te-Se system, we have developed a one-dimensional cluster expansion (CE) based on first-principles electronic structure calculations, which accounts for the Bi and Sb bilayer formation. Excellent interlayer distances are obtained with a van der Waals density functional. It is shown that a CE solely based on pair interactions is sufficient to provide an accurate description of the ground-state energies of Bi-Sb-Te-Se binary and ternary systems without making the data set of *ab initio* calculated structures unreasonably large. For the binary alloys $A_{1-x}Q_x$ (A = Sb, Bi; Q = Te, Se), a ternary CE yields an almost continuous series of (meta)stable structures consisting of consecutive A bilayers next to consecutive A_2Q_3 for $0 < x < 0.6$. For $x > 0.6$, the binary alloy segregates into pure Q and A_2Q_3. The Bi-Sb system is described by a quaternary CE and is found to be an ideal solid solution stabilized by entropic effects at $T \neq 0$ K but with an ordered structure of alternating Bi and Sb layers for $x = 0.5$ at $T = 0$ K. A quintuple CE is used for the ternary Bi-Sb-Te system, where stable ternary layered compounds with an arbitrary stacking of Sb_2Te_3, Bi_2Te_3, and Te-Bi-Te-Sb-Te quintuple units are found, optionally separated by mixed Bi/Sb bilayers. Electronic properties of the stable compounds were studied taking spin-orbit coupling into account.

DOI: 10.1103/PhysRevB.89.054106 PACS number(s): 31.15.A−, 61.50.Ah, 71.20.−b

I. INTRODUCTION

Bi-Sb-Te-Se alloys have been intensively studied during the last decades because of their interesting and technological important properties. They are not only excellent thermoelectric materials [1,2] but Sb-Te alloys have also attracted attention as a phase change material for the new generation of optical disks and nonvolatile random access memory [3]. Moreover, Bi_2Te_3, Bi_2Se_3, Sb_2Te_3, and $(Bi_xSb_{1-x})_2Te_3$ have been demonstrated to be topological insulators [4–7] and recently $Bi_{2-x}Sb_xTe_{3-y}Se_y$ solid solutions have been synthesized at various compositions to optimize the bulk-insulating behavior in topological insulators [8]. The best known and most studied compounds are A_2Q_3 (with A = Bi, Sb and Q = Te, Se), but varying the composition shows that the binary alloys $(A_{1-x}Q_x)$ exhibit a rich phase diagram with many stable structures in the range between $x = 0$ (elemental A) and $x = 0.60$ (A_2Q_3) [9]. A_2Q_3 (excluding Sb_2Se_3) crystallizes in a layered structure with rhombohedral lattice symmetry (space group $R\bar{3}m$). The hexagonal unit cell consists of three quintuple units with the sequence Q-A-Q-A-Q as illustrated in Fig. 1. The bonding between adjacent quintuple units is rather weak and of the van der Waals (vdW) type, whereas the bonding within the layers is of a covalent/ionic nature. All experimentally known A-rich phases (i.e., with more than 40% of A) can be classified according to the homologous series $(A_2)_n(A_2Q_3)_m$ with a stacking of A bilayers and A_2Q_3 units [10–16]. The hexagonal unit cells of the three most-widely known structures of this homologous series are shown in Fig. 1. The $(A_2)_n(A_2Q_3)_m$ compounds crystallize according to the rhombohedral (space group $R\bar{3}m$) or hexagonal lattice (space group $P\bar{3}m1$). First-principles electronic structure calculations within the density functional theory (DFT) formalism have been used to study the chemical bonding and electronic properties of several Bi-Se compounds demonstrating the small formation energy with respect to elemental A and A_2Q_3 [17].

In previous work, we have investigated systematically the phase stability at $T = 0$ K of the binary alloy $Sb_{1-x}Te_x$ for arbitrary composition x by means of DFT calculations and the cluster expansion (CE) technique thereby showing that a continuous series of (meta)stable ordered structures exists, a situation which is reminiscent of the infinitely adaptive structures introduced by Anderson [18]. The obtained structures consist of consecutive Sb bilayers next to consecutive Sb_2Te_3 units, with the general formula $(Sb_2)_n(Sb_2Te_3)_m$ with n and $m = 0,1,2,\ldots$ [19]. Since thermoelectric materials are often based on solid solutions [1,20], superstructures [21], or nanostructures [22] of Sb_2Te_3 and Bi_2Te_3 or of Bi and Sb [23,24], we will now look for the stable layered phases within the ternary Bi-Sb-Te system for an arbitrary composition by extending the methods used in Ref. [19]. The present method provides insight into the actual ground and metastable states, though it does not yield complete information on the finite temperature stability.

The CE technique [25] based on DFT calculations is used to study the energetics of arbitrary stackings of Bi, Sb, and Te layers. In order to account for the weak vdW interaction between the A_2Q_3 quintuple units, all calculations include the vdW functional proposed by Dion *et al.* [26]. An efficient implementation of this nonlocal correlation functional makes the calculations only slightly harder than traditional local or semilocal exchange and correlation (xc) functionals [27]. Both structural and electronic properties of (meta)stable phases are further analyzed by considering some of the representative structures.

*kirsten.govaerts@ua.ac.be

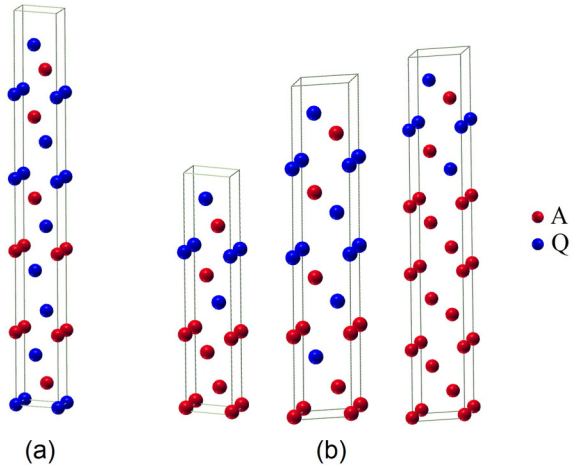

FIG. 1. (Color online) (a) Hexagonal unit cell of the stable A_2Q_3 structure. (b) Other experimentally observed structures $A_4A_2Q_3$, $A_2(A_2Q_3)_2$, and $A_{10}A_2Q_3$, respectively.

The paper is organized as follows. In Sec. II, we explain in more detail the implementation of the CE method used in this paper, and in Sec. III, we provide some technical details of the DFT calculations. In Sec. IV A, the results on the binary systems Bi-Te, Bi-Se, and Sb-Te are discussed, whereas in Sec. IV B, we address Bi-Sb. The ternary system Bi-Sb-Te is considered in Sec. IV C. Finally, we summarize our results in Sec. V.

II. METHODOLOGY

The main goal of this work is to understand and predict the most stable layered structures of the binary and ternary systems (at $T = 0$ K) consisting of Bi, Sb, Te, or Se. Since it is computationally very demanding to calculate the formation energy of all possible configurations with *ab initio* techniques, the CE method is used to find ground-state structures. Here, one only needs the accurately calculated energies of a relatively small number of structures in order to obtain the approximate energies of all possible configurations. The hexagonal structures investigated in this work have a fixed underlying fcc lattice with an ABCABC... stacking of the [111] planes, each plane containing only one type of atom. In the CE method, one starts from a one-to-one correspondence between the configuration of a compound and this fixed underlying lattice. Since we only consider the ordering of Bi, Sb, Te, and Se *layers*, a structure s is completely defined by a certain sequence of layers, so we can refer to a one-dimensional CE. The distinct layers are represented by occupation variables Γ_i^P, where i and P represents the layer and the atomic species, respectively, and which are defined by [25,28]

$$\Gamma_i^P = \begin{cases} 1 & \text{if layer } i \text{ is occupied by atomic type } P, \\ 0 & \text{otherwise.} \end{cases}$$

This definition is not the usual Ising selection, but as explained in Ref. [29], there is a straightforward conversion of cluster expansion coefficients between cluster expansions obtained with different choices for the occupation variables.

In Ref. [19], we showed that for the binary Sb-Te system, a converged binary CE of the formation energy cannot be realized with a dichotomous occupation variable Γ_i^P since no discrimination is made between an odd or an even number of adjacent Sb layers. The energetic difference between structures with an even or odd succession of Sb layers is a consequence of the strong structural relaxations accompanying a Peierls transition leading to the formation of Sb bilayers. Instead of further increasing the number of input structures, or making use of more elaborate techniques (e.g., the mixed-basis CE) to account for the strong relaxations [30,31], we implemented a ternary CE. The Sb atom is then given a different occupation variable depending on whether it is part of an even or an odd sequence of Sb layers, and another distinct occupation variable for Te. This ternary CE accounts explicitly for the bilayer formation and is able to discriminate between structures with an even or odd number of successive Sb layers, which was not the case for the binary CE. Since Bi and Se are expected to behave in a similar way to Sb and Te, respectively, a ternary CE will also be used for the Bi-Te and Bi-Se alloys. In order to account for the possible bilayer formation in the Bi-Sb and the Bi-Sb-Te system a quaternary and quintuple CE were developed, respectively. Two distinct occupation variables for both Bi and Sb are introduced, depending on whether they are part of an odd or even number of adjacent Bi and Sb layers together, and a fifth variable is used for Te.

The formation energy for a given structure s—or in fact any material property depending on the atomic configuration—can be written as an expansion of these occupation variables [25]

$$E^s_{\text{form}} = V_0 + \sum_P \sum_i V_i^P \Gamma_i^P + \sum_{P,P'} \sum_{i,j} V_{ij}^{P,P'} \Gamma_i^P \Gamma_j^{P'} + \cdots, \tag{1}$$

where the atomic type P now not only represents the atomic species, but is also different for Bi and Sb, depending on whether they are part of an odd or an even sequence of layers. The formation energy of a certain alloy is defined by

$$E^s_{\text{form}} = E^s - \sum_{\text{A}} \text{c}^s_{\text{A}} E_{\text{A}},$$

where E^s is the total energy per atom of configuration s and the sum runs over all different elements A of the compound, with E_{A} the energy of elemental A, and c_{A} the concentration of the element A in the specific configuration s.

The expansion coefficients $V_{ij\ldots}^{P\ldots}$ of Eq. (1) are the so-called effective cluster interactions (ECIs) and represent the relative importance of a specific grouping of layers, which can be nearest-neighbor layers, next nearest neighbor layers, but also one and no layer. These groupings of layers are called "clusters." A cluster α is not only characterized by its layers $i, j, \ldots$, but also by the atomic type $P, P', \ldots$ occupying these layers. Equation (1) can now be written as an expansion in terms of clusters α

$$E^s_{\text{form}} = \sum_\alpha V^\alpha \prod_{\substack{i \in \alpha \\ P \text{ on } i}} \Gamma_i^P. \tag{2}$$

The CE of Eq. (2) is, in principle, exact when all clusters are considered, but in practice, often only a limited number of

clusters is necessary to adequately represent the energy. When the CE is truncated by selecting only a few clusters, one can find the ECIs by solving Eq. (2) with a least-squares procedure (a generalization of the Connolly-Williams approach [32]), hereby using the energies calculated from first-principles for a relatively small number of configurations S,

$$\sum_{s=1}^{S} w^s \left[E^s_{\text{form,DFT}} - \sum_{\alpha} V^{\alpha} \prod_{\substack{i \in \alpha \\ P \text{ on } i}} \Gamma_i^P \right]^2 = \min,$$

with $E^s_{\text{form,DFT}}$ the *ab initio* computed formation energy of configuration s. Once the ECIs are known, Eq. (2) can be used to predict the formation energy of an arbitrary configuration at any concentration.

A weight factor is assigned to every structure, defined by [28]

$$w^s = \frac{1}{1 + \omega\left(\frac{d^s}{\langle d \rangle}\right)},$$

where d^s is the formation energy difference between structure s and the convex hull (which connects the energy values of the most stable, i.e., lowest energy, structures) for a given composition, $\langle d \rangle$ is the mean value of these energy differences taken from all structures. Here, we have chosen $\omega = 1$. This weight factor attributes a larger weight to the structures on or near the convex hull and a smaller weight to structures far away from the convex hull, which are less stable.

To determine the clusters that should be included in the CE, we took into account the results of Ref. [29], where it was shown that all subclusters of a considered cluster must be included in order to make the CE invariant with regard to the definition of the occupation variable. Since the CE is a tool to predict energies of new configurations, a measure for the accuracy of the CE prediction is needed. This measure is given by the leave-one-out-cross validation (LOOCV) [33,34], which is defined by

$$\text{LOOCV} = \sqrt{\frac{1}{S} \sum_{s=1}^{S} \left(E^s_{\text{form,DFT}} - E^{s*}_{\text{form,CE}} \right)^2}$$

with S the number of structures, $E^s_{\text{form,DFT}}$ the *ab initio* computed formation energy of configuration s and $E^{s*}_{\text{form,CE}}$ the CE-predicted formation energy, where the ECIs of this CE are calculated from a least-squares fit based on the initial input data set with the exclusion of the sth structure. Optimization of the LOOCV over all permutations of cluster combinations yields a "best" CE.

When the CE predicts a new ground-state structure, its formation energy will be situated below the convex hull. To find out whether this is really a ground-state structure, the formation energy has to be calculated with *ab initio* techniques and added to the initial data set of structures. A new CE has to be generated and the whole procedure starts over again. When no new ground states are found and the LOOCV has reached an acceptably small value (<20 meV/atom), convergence of the CE is reached. The weight factors w^s discussed above are introduced to accelerate this convergence.

III. COMPUTATIONAL DETAILS

Lattice parameters and atomic positions were optimized by relaxing the hexagonal Bi-Sb-Se-Te structures using first-principles calculations performed within the DFT formalism as implemented in the Vienna *ab initio* simulation package VASP [35,36]. We used the all-electron projector augmented wave (PAW) method with the Bi ($6s^2 6p^3$), Sb ($5s^2 5p^3$), Te ($5s^2 5p^4$), and Se ($4s^2 4p^4$) electrons treated as valence electrons. For the exchange and correlation functional, we considered the generalized gradient approximation of Perdew-Burke-Ernzerhof (PBE) [37] and took into account the vdW effect by using the vdW density functional (vdW-DF) as implemented in the VASP code [38]. In particular, we have used the so-called optB86b-vdW functional, which provides superior values for the lattice constants in comparison with other vdW-DF functionals (for a detailed discussion on the performance of the different functionals we refer to Refs. [38,39]).

For total energy calculations and structure optimization, a plane-wave cutoff value of 250 eV was chosen and a $16 \times 16 \times \ell$ grid [40] for the Brillouin zone integration, with ℓ depending on the c lattice parameter of the hexagonal unit cell; for three monolayers $\ell = 8$, for six monolayers $\ell = 4$, for nine monolayers $\ell = 3$, etc. With these settings, our results are converged within 10^{-4} eV/atom. For the electronic structure calculation we considered the results as converged when the energy difference between two successive steps was smaller than 10^{-5} eV and for the geometry optimization we considered a convergence criterium for the forces on the atoms of less than 10^{-3} eV/Å. To avoid that the atoms get trapped in local minima, all atoms were subjected to small random displacements from their initial fcc-lattice sites. Since for heavier elements the spin-orbit coupling (SOC) becomes important, all band structure calculations include this coupling.

IV. RESULTS AND DISCUSSION

As mentioned in Sec. II, fast convergence of the CE for the Sb-Te system can be achieved by considering a ternary CE where Sb atoms are given a different occupation variable depending on whether they are part of an even or odd number of adjacent Sb layers. In this way, the CE method takes into account the favoring of Sb bilayer formation [19]. Since Bi and Se are expected to behave in a similar way to Sb and Te, respectively, a ternary CE was used for the Bi-Te and Bi-Se alloys (Sec. IV A), while a quaternary and quintuple CE was used for the Bi-Sb (Sec. IV B) and Bi-Sb-Te (Sec. IV C) systems, respectively.

A. Binary systems Bi-Te, Bi-Se and Sb-Te

For the three systems Sb-Te, Bi-Te, and Bi-Se, a converged CE with only pair interactions was found with a data set of 72, 79, and 77 structures, respectively, and including not more than seven distinct (i.e., symmetrically nonequivalent and not depending on atom type) clusters with atom distances up to seven interplanar distances. In contrast to our previous work [19] where we used three-site clusters, we have shown in the present work that a CE solely based on pair interactions yield a converged CE. For details on this CE, see Ref. [41].

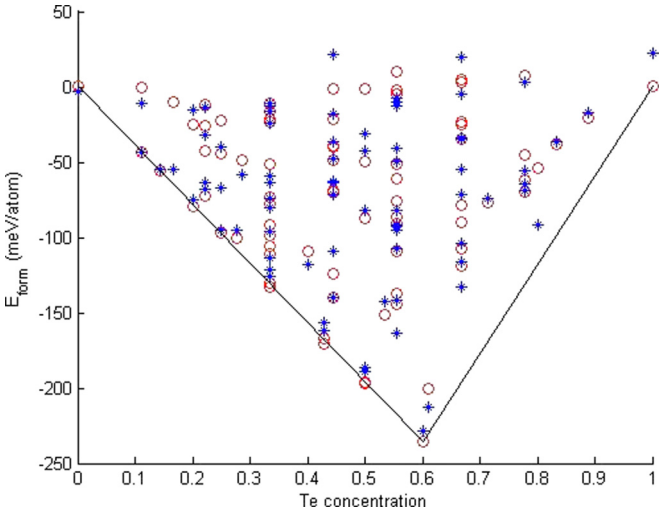

FIG. 2. (Color online) Formation energies of a data set of 79 Bi-Te layered structures, calculated by *ab initio* techniques (red circles) and predicted by the CE (blue stars). The convex hull is indicated by the full black lines.

In Fig. 2, the final *ab initio* data set for the Bi-Te system (79 structures) is shown together with the predicted values for the formation energies by the converged CE. In Fig. 3, we used this CE to generate the formation energy of $\sim 10^4$ Bi-Te layered structures.

For all three systems, a series of multilayered structures with an even number of successive Bi or Sb layers adjacent to successive units of Sb_2Te_3, Bi_2Te_3, and Bi_2Se_3 are found to be new groundstates in the region with $0 \leqslant x \leqslant 0.6$ (with x being the Te concentration). The general composition can therefore be written as $(A_2)_n(A_2Q_3)_m$, in line with the existing experimental [11–13,15,42] and computational data [17,19]. This does not exclude, however, that other layered structures with higher formation energy are observed at higher temperatures [16]. For $x > 0.6$, no stable compounds are found and the alloy segregates into A_2Q_3 and pure Q.

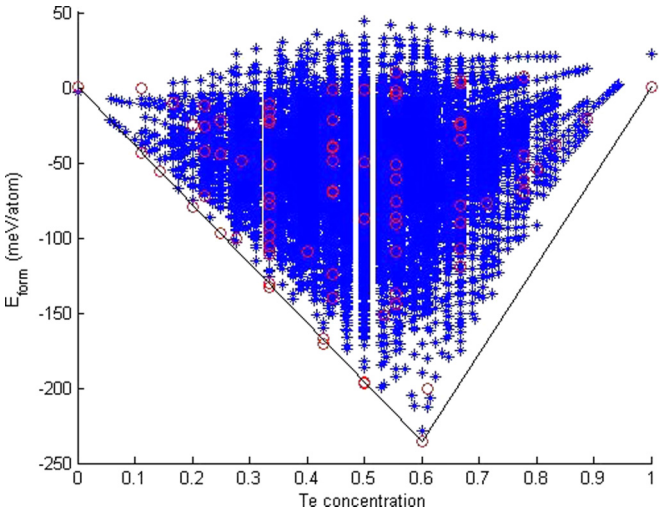

FIG. 3. (Color online) Predicted energies by the CE of $\sim 10^4$ layered structures (blue stars).

TABLE I. Interlayer distances and lattice parameters for the ground-state structures $(A_2)_4(A_2Q_3)_2$. The first four columns show the distance between two A layers in a bilayer, between two bilayers, between a bilayer and a quintuple unit and between two quintuple units respectively. The fifth column represents the size of a quintuple unit, i.e., the interplanar distance between the first and the last Q layers. Lattice parameters a and c/n (with n being the number of monolayers) can be found in the last two columns. All values are given in angstroms.

	A-A	A_2-A_2	A_2-A_2Q_3	A_2Q_3-A_2Q_3	A_2Q_3	a	c/n
Sb-Te	1.54	2.36	2.54	2.86	7.34	4.36	1.99
Bi-Te	1.67	2.39	2.40	2.64	7.40	4.49	2.01
Bi-Se	1.74	2.51	2.27	2.44	6.62	4.35	1.93

We have investigated interlayer distances and lattice parameters of a large number of stable compounds and on comparing the three binary systems Sb-Te, Bi-Te, and Bi-Se, we observe some obvious trends. As an example we give some specific distances for the optimized structures $(A_2)_4(A_2Q_3)_2$ in Table I. As expected for larger atoms, the distances between Bi (Te) layers are larger than those between Sb (Se) layers. Also the size of the quintuple units containing Te atoms is larger than that of the Bi_2Se_3 quintuple unit.

Since the vdW interaction is known to be important in the investigated systems, all structures were optimized with a vdW-DF for obtaining lattice parameters and interlayer distances in close agreement with experiment. In particular, this functional reduces the interlayer distance between two quintuple units with 4% to 12% in comparison with the results from a standard calculation with the semilocal PBE xc functional. This can be clearly seen in Table II where we show the optimized lattice parameters of A_2Q_3 structures with the regular PBE xc functional and with the vdW-DF, and compare them with the experimental results.

In order to illustrate the interaction of the vdW-DF on the electronic charge distribution, Fig. 4 shows an isosurface of the difference in charge density of $(Sb_2)_4(Sb_2Te_3)_2$, calculated with and without the vdW-DF. This structure is optimized using the vdW-DF, and a self-consistent calculation (with and without vdW-DF, respectively) was performed on this structure with fixed lattice parameters and atom positions. A small and spherically symmetric depletion of electrons occurs around all the atoms when including the vdW contribution. Between the quintuple units, the vdW contribution leads to a large nonspherical excess of electrons indicating its importance between these layers. We also observe a smaller excess of electrons between the bilayers and between a bilayer and a quintuple unit due to the vdW functional, as shown in Fig. 4. This increase indicates that the bonding between two bilayers, and between a bilayer and a quintuple unit is also of the weak vdW type.

Taking into account SOC, the band structure calculation shows that all structures of the homologous series $(A_2)_n(A_2Q_3)_m$ are semimetals (but with a small band overlap, ranging from 10 to 170 meV), except for A_2Q_3, which are semiconducting [44]. The electronic structure of A_2Q_3 has been intensively investigated in the (recent) past both because

TABLE II. Lattice parameters and interlayer distance between two quintuple units A_2Q_3 for the stable compounds A_2Q_3 for the three systems. A comparison between the relaxed structural parameters, with the PBE functional, the vdW functional, and the experimental values. All values are given in angstroms.

	PBE			vdW			exp [43]		
	a	c	A_2Q_3-A_2Q_3	a	c	A_2Q_3-A_2Q_3	a	c	A_2Q_3-A_2Q_3
Sb_2Te_3	4.335	31.398	3.074	4.312	30.351	2.709	4.264	30.458	2.829
Bi_2Te_3	4.446	32.023	3.128	4.413	30.823	2.720	4.386	30.497	2.625
Bi_2Se_3	4.187	30.893	3.270	4.162	28.884	2.595	4.143	28.636	2.579

of its thermoelectric properties [21] and its behavior as a topological insulator [45]. Since for heavier elements, SOC can significantly alter the band structure, we calculated the fundamental band gap for A_2Q_3 (after structural optimization) both with and without SOC and compared our results with the experimental values. This is shown in Table III. While the band-structure calculation without SOC gives direct fundamental band gaps at the Γ point, the fundamental band gaps calculated with SOC are indirect. For Sb_2Te_3, the SOC leads to a significant increase of the band gap, whereas in Bi_2Te_3 it is reduced by 50%. The band gap of 0.23 eV for Bi_2Se_3 remains unaltered by the inclusion of the SOC, which is in line with a previous calculation [46]. Since experimental band gaps often refer to the optical gap we include in Table III the direct gap values. Our result for Bi_2Te_3 is in excellent agreement with experiment [47,48], which might be fortuitous in view of the well-known underestimation of the band gap by DFT. The indirect nature of the calculated band gap seems to agree with experiment for Bi_2Te_3 [45] and Sb_2Te_3 [49], but there is recent experimental and theoretical evidence that Bi_2Se_3 has a direct band gap at the Γ point [50].

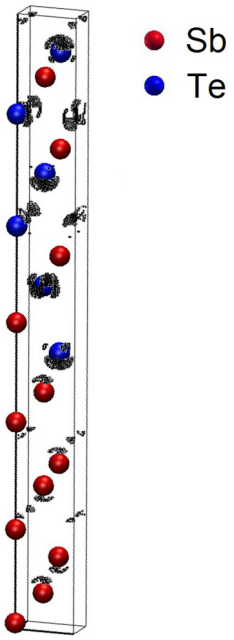

FIG. 4. (Color online) An isosurface of the small excess (0.0061 electrons/Å) of charge density between the calculations done with and without vdW-DF of the structure $(Sb_2)_4(Sb_2Te_3)_2$.

B. Binary system Bi-Sb

$Bi_{1-x}Sb_x$ alloys are known to form a solid solution over the entire composition range with a rhombohedral unit cell [52,53]. They are in general semimetallic with the exception of the range $0.07 < x < 0.22$ where they are semiconducting with a narrow band gap. The maximum band gap is approximately 20 meV and is reached for $x \sim 0.15$ [54]. In this section, we investigate the stability of layered structures at T = 0 K. In analogy with the previous binary systems, the occupation variable accounts for the fact that Bi or Sb belongs to an odd or even number of layers (irrespective of whether this is a Bi or Sb layer). A converged quaternary CE based on only pair interactions was found with a data set of 69 structures and which includes six distinct clusters with atom distances up to 4 interplanar distances. For details on this CE, see Ref. [41]. Figures 5 and 6 show the convex hull for the initial data set and the prediction for $\sim 10^4$ structures, respectively. From these results, it is clear that structures with an odd number of layers are less stable than structures with an even number of layers. This is again a consequence of the tendency to form bilayers due to the Peierls transition.

This convex hull shows that the formation energy of the Bi-Sb structures with an even number of layers is very small (<10 meV/atom). For completeness we compare the formation energy of the generated ordered structures with that of their disordered counterparts. To model the solid solution we created a $3 \times 3 \times 1$ supercell with six layers in the unit cell. Each layer contains nine lattice sites that are randomly occupied by Bi or Sb atoms. In total, we optimized 25 random structures for which the formation energy is added to Fig. 5. The considered structures still form bilayers and their formation energy is comparable to that of the fully ordered structures. At finite temperatures, the configurational entropy

TABLE III. Calculated band gaps (in eV) of the three stable compounds Sb_2Te_3, Bi_2Te_3, and Bi_2Se_3, without and with SOC taken into account, compared with the experimental values. For calculations without SOC, the band gap is direct, while for calculations with SOC, the fundamental band gap is indirect.

		With SOC		
	Without SOC	Indirect	Direct	Exp
Sb_2Te_3	0.01	0.12	0.14	0.15–0.28 [47,51]
Bi_2Te_3	0.31	0.16	0.16	0.16 [47,48]
Bi_2Se_3	0.23	0.23	0.27	0.33 [47,48]

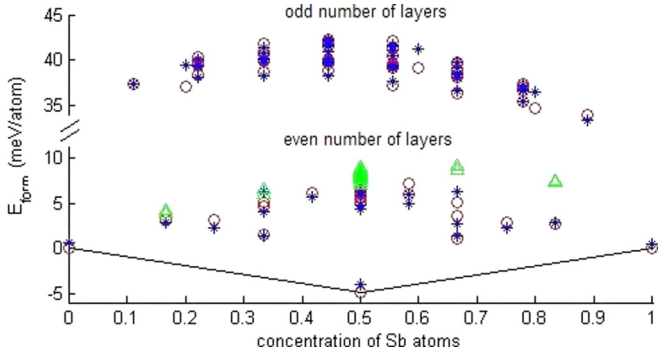

FIG. 5. (Color online) Formation energies of a data set of 69 Bi-Sb layered structures, calculated by *ab initio* techniques (red circles) and predicted by the CE (blue stars). Formation energies of structures with Bi and Sb atoms randomly distributed over the lattice sites, are denoted by green triangles. The convex hull is indicated by the full black lines.

will dominate and the Bi-Sb alloys can be considered as *almost* ideal solutions, which is in line with the experimental results [52,53]. However, at $T = 0$ K, a stable structure at 50 at.% is found, consisting of alternating Bi and Sb layers. This structure has lattice parameters $a = 4.46$ Å and $c = 11.57$ Å. The distance between two layers within the bilayer is 1.60 Å, while the distance between two bilayers is 2.26 Å. We notice that the lattice parameters of the stable Bi-Sb compound at 50 at.% obey Vegard's law, as shown in Table IV.

Our calculations were not able to reproduce the small band gap experimentally found for the composition range $0.07 < x < 0.22$ [54]. In fact all investigated structures (ordered and disordered), apart from the ordered structure at 50 at.%, were found to be semimetallic. This might be due to the fact that the observed band gap is small (∼20 meV) and therefore sensitive to small deviations in lattice parameters and the approximate nature of the xc functional in general (e.g., underestimation of the band gap). In Fig. 7, the band structure (including SOC) of the stable compound $Bi_{0.5}Sb_{0.5}$ is shown. This specific configuration shows semiconducting behavior with a band gap of 0.104 eV, which is significantly larger than the experimentally observed band gap of ∼20 meV in $Bi_{1-x}Sb_x$ solid solutions with $0.07 < x < 0.22$.

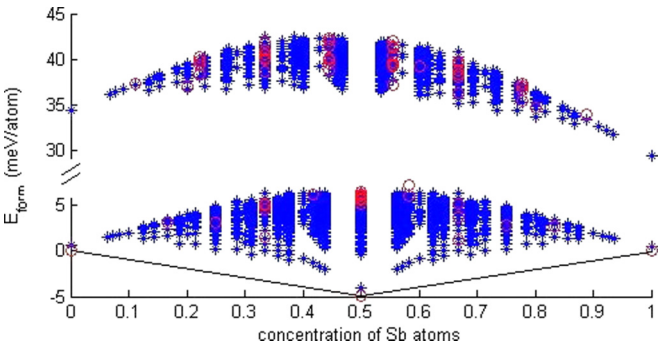

FIG. 6. (Color online) Predicted energies by the CE of $\sim 10^4$ layered structures (blue stars).

TABLE IV. Lattice parameters, intra- and interbilayers distances for the optimized structures of elemental Bi, Sb, and for the stable structure $Bi_{0.5}Sb_{0.5}$, with alternating Bi and Sb layers. All values are given in angstroms.

	a	c	Intrabilayer	Interbilayer
Bi	4.55	11.83	1.65	2.30
Sb	4.36	11.29	1.54	2.22
Mean value	4.46	11.56	1.60	2.26
BiSb	4.46	11.57	1.60	2.26

C. Ternary system Bi-Sb-Te

Since thermoelectric materials often consist of more than just two elements from the series Bi, Sb, Te, Se, we apply in this section the CE technique to investigate the ternary Bi-Sb-Te system (the ternary Bi-Sb-Se system is expected to behave similarly). The formation of homologous series consisting of layered structures for the binary subsystems A-Q (A = Bi, Sb; Q = Te, Se) suggests that stable layered ternary compounds may be formed. To anticipate on the formation of bilayers we introduce a CE with five occupation variables: two for both Bi and Sb, depending on whether they are part of an odd or an even number of adjacent Bi and/or Sb layers, and a fifth for Te. To obtain a converged CE, more than 400 structures were needed, seven distinct clusters were included, with interlayer distances up to six. For details on this CE, see Ref. [41]. Again, we remark that the CE only uses pair interactions to describe accurately the formation energies of the layered ternary alloys. The formation energy for $\sim 10^7$ structures as a function of the Bi and Sb concentration is shown in Fig. 8 with the 3D convex hull. As expected, the quintuple CE reproduces the results for the binary subsystems discussed in Secs. IV A and IV B with the homologous series $(Sb_2)_n(Sb_2Te_3)_m$ and $(Bi_2)_n(Bi_2Te_3)_m$ and the stable BiSb compound.

Genuine ternary ground-state structures are obtained for unit cells built up from an arbitrary stacking of the three quintuple units Sb_2Te_3, Bi_2Te_3, and Te-Bi-Te-Sb-Te. For a specific concentration, different stackings of these quintuple units are possible, but their energies differ by no more than 0.5 meV/atom and should therefore be considered as degenerate. This result and the results of Sec. IV B on random Bi-Sb structures suggest that Bi and Sb can be randomly interchanged. To investigate the stability of structures with

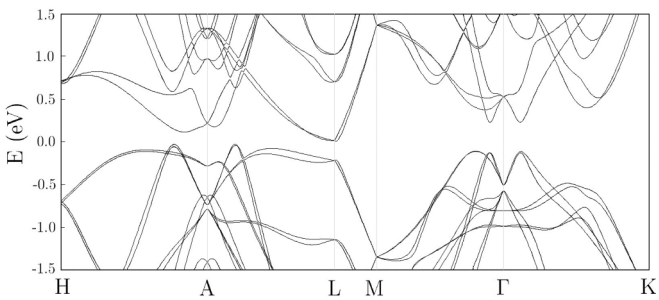

FIG. 7. The band structure of $Bi_{0.5}Sb_{0.5}$ with alternating Bi and Sb layers. Energy values are with respect to the top of the valence band.

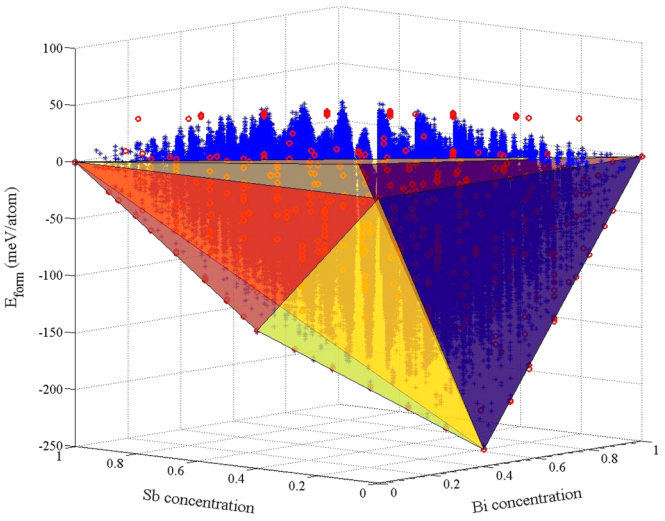

FIG. 8. (Color online) Predicted energies by the CE of $\sim 10^7$ layered structures (blue stars). Red circles denote the initial input data set of 432 *ab initio* calculated energies.

Bi and Sb at random positions in the quintuple units, we created a $3 \times 3 \times 1$ supercell with 15 atoms in the unit cell. This supercell contains three quintuple units, and each layer contains nine lattice sites, which are fully occupied by Te or randomly occupied by Bi or Sb. With energy differences of no more than 0.5 meV/atom, we conclude that structures with a random composition of Bi and Sb within a monolayer should also be considered as structures degenerate with the corresponding (i.e., for the same concentration of Bi and Sb) stacking of monolayers.

In Table V, we show the band gaps (including SOC) of some of these groundstate structures, for different concentrations of Bi. Degenerate structures for a given concentration yield the same band gap.

Other stable (or slightly metastable) compounds are found when an excess of Bi and/or Sb is present. These structures consist of an even number of Bi and/or Sb layers, next to quintuple units of Bi_2Te_3 and have formation energies ranging from 0 to 13 meV/atom above the convex hull. Again, we compared these energies with the formation energies of their random counterparts. Therefore we created a $3 \times 3 \times 1$ supercell with 15 layers in the unit cell: five for the quintuple unit and ten for the bilayers. In a first case, Bi and Sb are randomly distributed in the bilayers, while the quintuple unit Bi_2Te_3 remains unaltered. These structures have formation energies in the above mentioned interval of 0 to 13 meV/atom above the convex hull, which implies that the Bi and Sb atoms are interchangeable in the bilayers, in line with the conclusions

TABLE V. Band gaps of several ternary ground-state structures consisting of adjacent quintuple units, for different concentrations of Bi.

Bi concentration	0.4 (Bi_2Te_3)	0.333	0.267	0.2	0.133	0.067	0 (Sb_2Te_3)
band gap (eV)	0.16	0.12	0.11	0.09	0.10	0.08	0.12

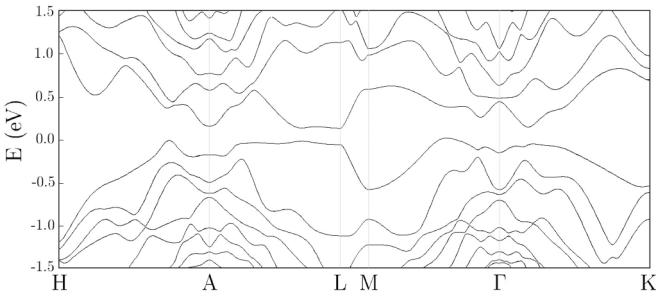

FIG. 9. The band structure of Bi-Sb-Sb-Bi(Bi_2Te_3).

of Sec. IV B. In a second case, the Bi layers in the quintuple unit are replaced by layers where Bi and Sb atoms are randomly interchanged, while the bilayers are entirely monoatomic. The formation energies of these structures can be found at 20 to 43 meV/atom above the convex hull. The structures consisting of other quintuple units with monoatomic layers (Sb_2Te_3 and Te-Sb-Te-Bi-Te) next to Bi and/or Sb bilayers can also be found in this range. These results suggest that structures with Bi_2Te_3 quintuple units are more likely to form. Furthermore, we created supercells where bilayers and Bi layers in the quintuple unit are now replaced by layers with randomly organized Bi and/or Sb atoms. These structures have energies again in the range of 20 to 43 meV/atom above the convex hull. For completeness, we also compared these energies with the energies of fully random structures, where the Te atoms are also replaced randomly. These structures are far less stable with formation energies of 100 meV/atom and more above the convex hull.

We examined the electronic structure (including SOC) of several ($\sim$20) stable or metastable compounds with an even number of Bi and/or Sb layers (ordered or disordered) next to Bi_2Te_3. Our results suggest that all compounds exhibit semimetallic behavior over the whole Sb concentration range, apart from some specific structures with an equal number of Sb and Bi atoms in the bilayers. Two illustrative examples are given by the layer sequences Bi-Sb-Sb-Bi(Bi_2Te_3) and (Bi-Sb)$_5$(Bi_2Te_3), which are semiconductors with a fundamental band gaps of 0.11 and 0.004 eV, respectively (both indirect). In Fig. 9, we give the full band structure of the former structure.

V. CONCLUSION

We have presented a systematic study of the stable layered structures at $T = 0$ K for the binary systems Bi-Te, Bi-Se (and Sb-Te) and Bi-Sb, and for the ternary alloy Bi-Sb-Te by means of a combination of the CE method and first-principles electronic structure calculations. In order to account for the existence of long-periodic layered structures and the strong structural relaxations, we developed a one-dimensional CE with occupation variables explicitly accounting for the fact that Sb or Bi atoms are part of an even or odd number of layers. Moreover, the use of a vdw-DF assures interlayer distances in excellent agreement with experiment are obtained. Accurate formation energies of binary and ternary layered alloys are obtained with CEs taking into account only a limited number of pair interactions.

For the binary systems $A_{1-x}Q_x$ (A = Sb, Bi; Q = Te, Se) the resulting stable structures for $x \leqslant 0.6$ are the homologous series $(A_2)_n(A_2Q_3)_m$ built up from successive bilayers A_2 and quintuple units A_2Q_3. For $x > 0.6$, the binary alloy segregates into pure Q and A_2Q_3. Apart from A_2Q_3, which is a semiconductor, all members of the homologous series turned out to be semimetallic in our SOC band structure calculation, though the band overlap is small for some of the studied compounds.

The $Bi_{1-x}Sb_x$ system is found to be an *almost* ideal solution, thermodynamically completely determined by the configurational entropy. At $T = 0$ K, however, a stable long-ranged ordered structure with a small negative formation energy is found at $x = 0.5$ at.% with alternating Sb and Bi layers. A band-structure calculation (with SOC) shows that this compound is a semiconductor with a band gap of 0.104 eV.

Finally, we have addressed the ternary Sb-Bi-Te system. The CE (based on ~400 *ab initio* results) not only reproduces the binary stable structures but also found stable ternary layered compounds with an arbitrary stacking of Sb_2Te_3, Bi_2Te_3, and Te-Bi-Te-Sb-Te quintuple units, optionally separated by mixed Bi/Sb bilayers. Our results allow for a direct link between composition and (electronic) structure for the binary and ternary Bi-Sb-Te systems and provide a starting point for the investigation of the phase stability at $T \neq 0$ K.

ACKNOWLEDGMENTS

We gratefully acknowledge financial support from the FWO-Vlaanderen through project G.0150.13. K.G. thanks the University of Antwerp for a PhD fellowship. This work was carried out using the HPC infrastructure at the University of Antwerp (CalcUA), a division of the Flemish Supercomputer Center VSC, supported financially by the Hercules foundation and the Flemish Government (EWI Department).

[1] F. D. Rosi, B. Abeles, and R. V. Jensen, J. Phys. Chem. Solids **10**, 191 (1959).
[2] G. J. Snyder and E. S. Toberer, Nat. Mater. **7**, 105 (2008).
[3] M. H. Lankhorst, B. W. Ketelaars, and R. A. Wolters, Nat. Mater. **4**, 347 (2005).
[4] H. J. Zhang, C. X. Liu, X. L. Qi, X. Dai, Z. Fang, and S. C. Zhang, Nat. Phys. **5**, 438 (2009).
[5] Y. Xia, D. Qian, D. Hsieh, L. Wray, A. Pal, H. Lin, A. Bansil, D. Grauer, Y. S. Hor, R. J. Cava, and M. Z. Hasan, Nat. Phys. **5**, 398 (2009).
[6] D. Kong, Y. Chen, J. J. Cha, Q. Zhang, J. G. Analytis, K. Lai, Z. Liu, S. S. Hong, K. J. Koski, S. K. Mo, Z. Hussain, I. R. Fisher, Z. X. Shen, and Y. Cui, Nat. Nanotechnol. **6**, 705 (2011).
[7] J. Zhang, C. Z. Chang, Z. Zhang, J. Wen, X. Feng, K. Li, M. Liu, K. He, L. Wang, X. Chen, Q. K. Xue, X. Ma, and Y. Wang, Nat. Commun. **2**, 574 (2011).
[8] Z. Ren, A. A. Taskin, S. Sasaki, K. Segawa, and Y. Ando, Phys. Rev. B **84**, 165311 (2011).
[9] In the present work, we do not consider the Sb-Se system.
[10] N. Kh. Abrikosov and M. M. Stasova, Inorg. Mater. **21**, 1758 (1985).
[11] L. E. Shelimova, O. G. Karpinskii, M. A. Kretova, V. I. Kosyakov, V. A. Shestakov, V. S. Zemskov, and F. A. Kuznetsov, Inorg. Mater. **36**, 768 (2000).
[12] P. M. Imamov and S. A. Semiletov, Kristallografiya **15**, 972 (1970).
[13] K. Kifune, Y. Kubota, T. Matsunaga, and N. Yamada, Acta Crystallogr. B **61**, 492 (2005).
[14] C. W. Sun, J. Y. Lee, M. S. Youm, and Y. T. Kim, Phys. Stat. Sol. (RRL) **1**, R25 (2007).
[15] C. W. Sun, J. Y. Lee, M. S. Youm, and Y. T. Kim, Jpn. J. Appl. Phys. **45**, 9157 (2006).
[16] N. Frangis, S. Kuypers, C. Manolikas, G. Van Tendeloo, J. Van Landuyt, and S. Amelinckx, J. Solid State Chem. **84**, 314 (1990).
[17] H. Lind, S. Lidin, and U. Hussermann, Phys. Rev. B **72**, 184101 (2005).
[18] J. S. Anderson, J. Chem. Soc., Dalton Trans. **10**, 1107 (1973).
[19] K. Govaerts, M. H. F. Sluiter, B. Partoens, and D. Lamoen, Phys. Rev. B **85**, 144114 (2012).
[20] B. Poudel, Q. Hao, Y. Ma, Y. Lan, A. Minnich, B. Yu, X. Yan, D. Wang, A. Muto, D. Vashaee, X. Chen, J. Liu, M. S. Dresselhaus, G. Chen, and Z. Ren, Science **320**, 634 (2008).
[21] R. Venkatasubramanian, E. Siivola, T. Colpitts, and B. O'Quinn, Nature (London) **413**, 597 (2001).
[22] Y. Q. Cao, X. B. Zhao, T. J. Zhu, X. B. Zhang, and J. P. Tu, Appl. Phys. Lett. **92**, 143106 (2008).
[23] G. E. Smith and R. Wolfe, J. Appl. Phys. **33**, 841 (1962).
[24] S. Tang and M. S. Dresselhaus, Phys. Rev. B **86**, 075436 (2012).
[25] D. de Fontaine, Solid State Phys. **47**, 33 (1994).
[26] M. Dion, H. Rydberg, E. Schröder, D. C. Langreth, and B. I. Lundqvist, Phys. Rev. Lett. **92**, 246401 (2004).
[27] G. Román-Pérez and J. M. Soler, Phys. Rev. Lett. **103**, 096102 (2009).
[28] M. H. F. Sluiter and Y. Kawazoe, Phys. Rev. B **68**, 085410 (2003).
[29] M. H. F. Sluiter and Y. Kawazoe, Phys. Rev. B **71**, 212201 (2005).
[30] D. B. Laks, L. G. Ferreira, S. Froyen, and A. Zunger, Phys. Rev. B **46**, 12587 (1992).
[31] O. Shchyglo, A. Diaz-Ortiz, A. Udyansky, V. N. Bugaev, H. Reichert, H. Dosch, and R. Drautz, J. Phys.: Condens. Matter. **20**, 045207 (2008).
[32] J. W. D. Connolly and A. R. Williams, Phys. Rev. B **27**, 5169 (1983).
[33] A. van de Walle and G. Ceder, J. Phase Equilib. **23**, 348 (2002).
[34] M. H. F. Sluiter, Y. Watanabe, D. de Fontaine, and Y. Kawazoe, Phys. Rev. B **53**, 6137 (1996).
[35] G. Kresse and J. Furthmüller, Comput. Mater. Sci. **6**, 15 (1996).
[36] G. Kresse and J. Furthmüller, Phys. Rev. B **54**, 11169 (1996).
[37] J. P. Perdew, K. Burke, and M. Ernzerhof, Phys. Rev. Lett. **77**, 3865 (1996).
[38] J. Klimes, D. R. Bowler, and A. Michaelides, Phys. Rev. B **83**, 195131 (2011).
[39] K. Govaerts, R. Saniz, B. Partoens, and D. Lamoen, Phys. Rev. B **87**, 235210 (2013).

[40] H. J. Monkhorst and J. D. Pack, Phys. Rev. B **13**, 5188 (1976).

[41] See Supplemental Material at http://link.aps.org/supplemental/10.1103/PhysRevB.89.054106 for a table containing the structures used for the CE with their *ab initio* calculated energies, and the clusters of this CE with their ECIs.

[42] M. S. Youm, Y. T. Kim, Y. H. Kim, and M. Y. Sung, Phys. Stat. Sol. (a) **205**, 1636 (2008).

[43] P. Villars and L. D. Calvert, *Pearson's Handbook of Crystallographic Data for Intermetallic Phases* (Asm International, Materials Park, Ohio, 1991).

[44] In a previous publication (see Ref. [19]), we found a transition from semimetallic to semiconducting behavior between 40 and 50 at.% Te in the $(Sb_2)_n(Sb_2Te_3)_m$ homologous series. However, these calculations were performed without the SOC.

[45] D. Hsieh, Y. Xia, D. Qian, L. Wray, F. Meier, J. H. Dil, J. Osterwalder, L. Patthey, A. V. Fedorov, H. Lin, A. Bansil, D. Grauer, Y. S. Hor, R. J. Cava, and M. Z. Hasan, Phys. Rev. Lett. **103**, 146401 (2009).

[46] S. K. Mishra, S. Satpathy, and O. Jepsen, J. Phys.: Condens. Matter. **9**, 461 (1997).

[47] D. L. Greenaway and G. Harbeke, J. Phys. Chem. Solids **26**, 1585 (1965).

[48] J. Black, E. M. Conwell, L. Seigle, and C. W. Spencer, J. Phys. Chem. Solids **2**, 240 (1957).

[49] W. Procarione and C. Wood, Phys. Status Solidi **42**, 871 (1970).

[50] I. A. Nechaev, R. C. Hatch, M. Bianchi, D. Guan, C. Friedrich, I. Aguilera, J. L. Mi, B. B. Iversen, S. Blügel, Ph. Hofmann, and E. V. Chulkov, Phys. Rev. B **87**, 121111 (2013).

[51] Landolt-Börnstein, *Numerical Data and Functional Relationships in Science and Technology*, edited by O. Madelung, M. Schulz, and H. Weiss, New Series, Group III, Vol. 17 (Springer, Berlin, 1983).

[52] W. F. Ehret and M. B. Abramson, J. Am. Chem. Soc. **56**, 385 (1934).

[53] P. Cucka and C. S. Barrett, Acta Cryst. **15**, 865 (1962).

[54] S. Cho, A. DiVenere, G. K. Wong, J. B. Ketterson, and J. R. Meyer, J. Appl. Phys. **85**, 3655 (1999).